Journal of Pathology
J Pathol 2001; **193**: 500–506.
DOI: 10.1002/path.897

Original Paper

Brain Aβ amyloidosis in APPsw mice induces accumulation of presenilin-1 and tau

Yasushi Tomidokoro[1]*, Yasuo Harigaya[1], Etsuro Matsubara[1], Masaki Ikeda[1], Takeshi Kawarabayashi[2], Tomoaki Shirao[3], Koichi Ishiguro[4], Koichi Okamoto[1], Steven G. Younkin[2] and Mikio Shoji[1]

[1] *Department of Neurology, Gunma University School of Medicine, Maebashi, Gunma 371-8511, Japan*
[2] *Department of Pharmacology, Mayo Clinic Jacksonville, Jacksonville, FL 32224, USA*
[3] *Department of Neurobiology and Behavior, Gunma University School of Medicine, Maebashi, Gunma 371-8511, Japan*
[4] *Project 8, Mitsubishi Kasei Institute of Life Sciences, Mimamiooya, Machida, Tokyo 194-8511, Japan*

*Correspondence to:
Yasushi Tomidokoro, MD, PhD,
Department of Neurology,
Gunma University School of
Medicine, 3-39-22 Showamachi,
Maebashi, Gunma 371-8511,
Japan.
E-mail:
tomidoko@med.gunma-u.ac.jp

Received: 14 September 2000
Accepted: 30 January 2001
Published online: 5 June 2001

Abstract

APPsw transgenic mice (Tg2576) overproducing mutant amyloid β protein precursor (βAPP) show substantial brain Aβ amyloidosis and behavioural abnormalities. To clarify the subsequent abnormalities, the disappearance of neurons and synapses and dystrophic neurite formation with accumulated proteins including hyperphosphorylated tau were examined. Tg2576 demonstrated substantial giant core plaques and diffuse plaques. The number of neurons was significantly decreased in the areas containing the amyloid cores compared with all other areas and corresponding areas in non-transgenic littermates in sections visualized by Nissl plus Congo red double staining ($p < 0.001$). The presynaptic protein α-synuclein and postsynaptic protein drebrin were also absent in the amyloid cores. βAPP and presenilin-1 were accumulated in dystrophic neurites in and around the core plaques. Tau phosphorylated at five independent sites was detected in the dystrophic neurites in the amyloid cores. Thus, the giant core plaques replaced normal brain tissues and were associated with subsequent pathological features such as dystrophic neurites and the appearance of hyperphosphorylated tau. These findings suggest a potential role for brain Aβ amyloidosis in the induction of secondary pathological steps leading to mental disturbance in Alzheimer's disease.

Keywords: **brain Aβ amyloidosis; βAPP; transgenic mice; presenilin-1; hyperphosphorylated tau; α-synuclein; drebrin; Alzheimer's disease**

Introduction

Alzheimer's disease (AD) is the most common neurodegenerative disorder in senile dementia. AD brains are characterized by two pathological features: initial Aβ amyloidosis by extracellular deposition of Aβ40 and Aβ42(43); and secondary tauopathy characterized by intracellular accumulation of neurofibrillary tangles (NFTs) composed of hyperphosphorylated tau, accompanied by loss of neurons and synapses. Since familial AD-linked mutations of amyloid β protein precursor (βAPP), presenilin-1 (PS-1), and presenilin-2 increase the extracellular concentration of Aβ42(43), this peptide is likely to be an initiating factor in the evolution of all types of AD [1]. Recent transgenic mouse studies revealed that overproduction of mutant βAPP causes substantial Aβ amyloid deposition and behavioural abnormalities [2], but the appearance of NFTs and loss of neurons and synapses have not yet been demonstrated [3]. The subsequent steps through initial Aβ amyloid deposition leading to such pathological changes remain to be clarified. In this study, we examined APPsw transgenic mice (Tg2576) and our findings can be summarized as follows: brain Aβ amyloidosis replaced brain tissue; dystrophic neurites were formed with accumulation of PS-1, βAPP, and α-synuclein; and hyperphosphorylated tau was detected.

Materials and methods

Twenty Tg2576 mice expressing $\beta APP695_{K595N/M596L}$ were examined at 4 ($n=2$), 8 ($n=4$), 10 ($n=4$), 12 ($n=6$), 15 ($n=2$), and 18 ($n=2$) months of age and compared with 20 age-matched control non-transgenic littermates [2]. The brain tissues were fixed in 4% paraformaldehyde with 0.1 M phosphate-buffered saline (pH 7.6) and embedded in paraffin wax. After formic acid pretreatment and blocking, sections 5 μm thick were incubated with primary antibodies. Specific labelling was visualized using a Vectastain Elite ABC kit (Vector, Burlingame, CA, USA) [4]. The antibodies used were anti-$A\beta_{40/42}$ antibody Mizuho [5], anti-$\beta APP_{666-695}$ antibody Saeko [4], anti-PS-1 antibodies (HS-C to PS-$1_{453-467}$, HSL-292 to PS-$1_{292-296}$, and HSN-2 to PS-1_{1-22}) [6], anti-tau antibodies specific to individual phosphorylation sites (anti-PS199 to phosphorylated Ser199, anti-PT205 to phosphorylated Thr205, anti-PT231PS235 to phosphorylated Thr231/Ser235, anti-PS396 to phosphorylated Ser396, and anti-PS413 to phosphorylated Ser413) [7,8], anti-α-synuclein antibodies (NACPN to α-synuclein$_{1-30}$ and NACPC to α-synuclein$_{111-140}$) [9], anti-drebrin monoclonal antibody M2F6 [10], and anti-ubiquitin antibody (Dakopatts, Glostrup, Denmark). Methenamine silver staining was performed to detect Aβ deposition

[11]. The total numbers of nuclei in 3×10^4 μm^2 fields of the temporal cortices with or without amyloid cores were counted in thioflavin S plus 1 μg/ml DAPI (4′,6-diamidine-2′-phenylindole dihydrochloride; Boehringer, Mannheim, Germany)-stained sections. The number of neurons in the temporal cortices was counted using Congo red plus Nissl- or Giemsa-stained sections [3,12]. Neurons and non-neuronal cells were counted separately in each of a series of four concentric circles around the amyloid cores [13]. The ring widths corresponded to the radii of the amyloid cores. For example, the innermost circle circumscribed the amyloid core. The fourth circle extended four core radii from the centre of the amyloid core. Cell numbers were also counted in corresponding areas without amyloid cores in the brains of Tg2576 and non-transgenic mice. One-way ANOVA and Bonferroni's multiple comparison test, or the Kruskal–Wallis test and Dunn's multiple comparison test were used for statistical analysis (Prism; GraphPad Software, San Diego, CA, USA).

Results

Abundant diffuse plaques and giant core plaques with spines were shown to be prominent in the cerebral cortex of Tg2576 by methenamine silver staining (Figure 1a). Giant core plaques did not have amyloid halos (Figure 1a; arrow). The diameters of the amyloid cores were approximately 15 to 150 μm, larger than those in the AD brain. Small amyloid cores clustered together and formed large senile plaques. In 18-month-old Tg2576 mice, approximately 70% of the plaques were diffuse plaques, which were small, perineural or large amorphous deposits ~100 μm in diameter. These diffuse plaques had the same appearance as those in the AD brain, showing no neuronal loss or dystrophic neurites (Figure 1a). Giant core plaques and diffuse plaques were distributed in the cerebral cortex, olfactory bulb, and hippocampus. No senile plaques were observed in the brainstem or cerebellum. Both types of plaques appeared simultaneously in the hippocampus and the temporal cortex at 8 months of age. The numbers of both types of plaques increased with age and eventually were eight-fold higher in 18-month-old mice than in 8-month-old mice.

In the giant amyloid core, no nuclei were observed in sections labelled by double staining with DAPI and thioflavin S (Figures 1b and 1c). Few nuclei were observed around the amyloid core. Neurons and non-neuronal cells seemed to disappear rather than being extruded by the core plaques. The number of nuclei was not preserved but was significantly decreased in areas including the core plaques compared with areas without such core plaques in the Tg2576 and control mouse cortex ($p < 0.001$; Figure 1d).

On Nissl and Giemsa staining, no neuronal or non-neuronal cells were found in the amyloid cores, in agreement with the results of DAPI staining (Figures 2a and 2b, arrow-heads). Around the amyloid core, only non-neuronal cells were observed. The appearance of neurons was preserved without compression by the amyloid core. Since focal neuronal loss might be induced in the vicinity of the core, the cell densities in four concentric areas centred on core plaques were calculated. Area 1 included the amyloid core, whereas areas 2–4 each extended one additional core radius from the centre so that the outside of the largest area was four core radii from the centre (Figure 2c). The number of neurons was significantly decreased in area 1 containing an amyloid core ($0.62 \pm 1.25/10^4$ μm^2, $n = 22$; mean ± SD) compared with all other areas (area 2: 12.13 ± 7.13, area 3: 13.83 ± 6.74, and area 4: $13.27 \pm 4.42/10^4$ μm^2, $n = 22$) and corresponding areas without core plaque in Tg2576 (area 1′: 20.66 ± 14.93, area 2′: 18.74 ± 7.80, area 3′: 16.88 ± 6.35, and area 4′: $16.17 \pm 6.22/10^4$ μm^2, $n = 22$) or in the non-transgenic brain (area 1″: 23.98 ± 14.16, area 2″: 20.62 ± 10.56, area 3″: 17.75 ± 10.02, and area 4″: $18.57 \pm 9.33/10^4$ μm^2, $n = 22$) in sections labelled with Nissl plus Congo red double staining ($p < 0.001$; Figure 2d). Since neurons were found in the space between the edge of the irregularly shaped amyloid core and the core-circumscribing circle, its final density was not zero in area 1. There were no significant differences in the densities of neurons within these areas, except area 1 in the Tg2576 or non-transgenic brain. In area 2, the density of neurons was not increased compared with areas 3 and 4. The numbers of neurons in area 2 did not compensate for the neuronal disappearance in area 1. The same findings were observed even if the core plaques were divided into two groups, i.e. layers 2–3 or layers 4–6 of the cerebral cortex. In contrast, non-neuronal cells counted in the same areas did not show significant differences among the areas examined (area 1: 8.97 ± 10.33, area 2: 13.23 ± 5.94, area 3: 8.48 ± 3.68, area 4: 8.14 ± 3.67; area 1′: 9.09 ± 7.31, area 2′: 8.51 ± 3.02, area 3′: 7.88 ± 4.86, area 4′: 8.89 ± 3.36; area 1″: 8.88 ± 7.85, area 2″: 10.75 ± 5.97, area 3″: 8.28 ± 3.79, and area 4″: $9.51 \pm 3.98/10^4$ μm^2, $n = 22$; Figure 2e). Corresponding to the decreased total nuclei count in the core plaque area observed by thioflavin S plus DAPI staining, the reduction of neurons caused decreased total cell counts in area 1 (area 1: 9.59 ± 11.04 vs. area 2: 25.73 ± 10.84, area 3: 22.50 ± 6.62, area 4: 21.41 ± 6.64; area 1′: 29.71 ± 13.11, area 2′: 27.25 ± 8.24, area 3′: 24.76 ± 7.72, area 4′: 25.03 ± 6.57; area 1″: 32.86 ± 13.33, area 2″: 31.37 ± 9.89, area 3″: 26.03 ± 9.77, and area 4″: $28.09 \pm 9.50/10^4$ μm^2, $n = 22$; $p < 0.001$; Figure 2f).

These amyloid cores were labelled by anti-Aβ antibody Mizuho (Figure 3a). In the hippocampus of 18-month-old mice, pyramidal cells of CA-1 and granular cells of the dentate gyrus were lost in the vicinity of the core plaques without compression of intranuclear distances (Figure 3a, arrow). The neuronal layers were thinner, although they were distant from the core plaques.

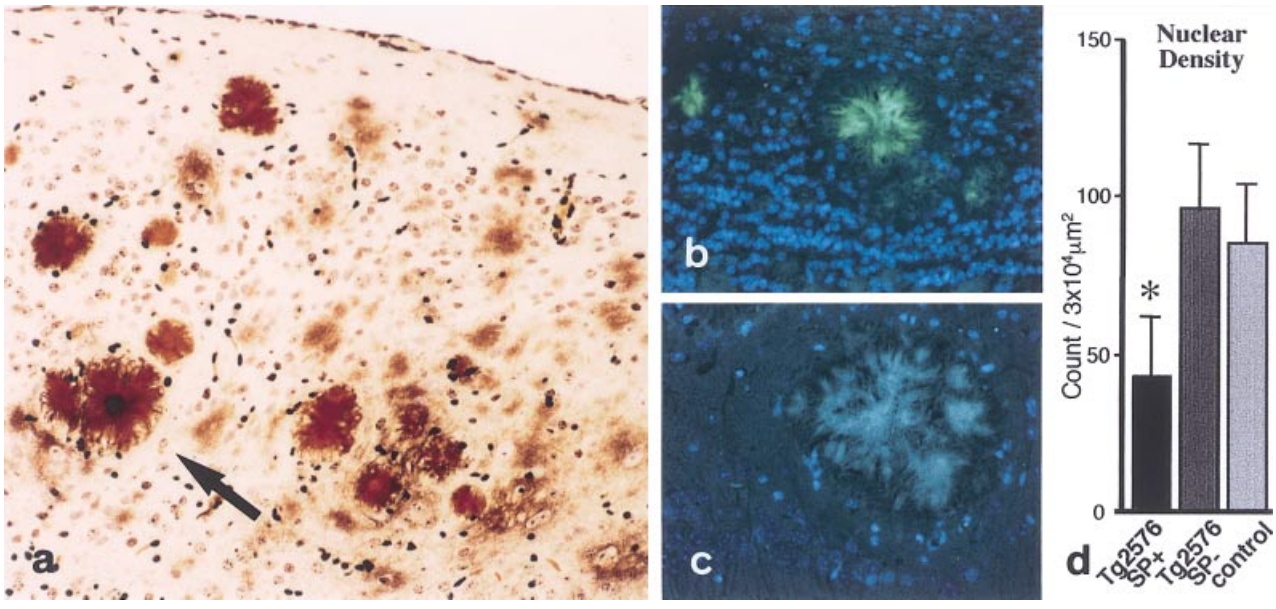

Figure 1. Methenamine silver staining of the temporal cortex (a) and double fluorescence staining by thioflavin S and DAPI of the olfactory bulb (b) and temporal cortex (c) of 18-month-old Tg2576 mice. The numbers of nuclei were counted in the temporal cortex of Tg2576 and non-transgenic mice by double fluorescence staining (d). (a) Abundant diffuse plaques and giant core plaques with spines (arrow) were prominent in the cerebral cortex. (b) Neuronal or non-neuronal cell nuclei were not detected by DAPI staining in or around the thioflavin S-positive core plaques. (c) In the hippocampus, pyramidal cells of CA-1 were lost in the vicinity of the core plaques. (d) Significant decreases in the number of nuclei were observed in the core plaque areas in the Tg2576 mouse brain (SP+; $42.7 \pm 19.2/3 \times 10^4$ μm^2), compared with areas without core plaques in the brains of Tg2576 (SP−; $95.6 \pm 20.8/3 \times 10^4$ μm^2) and control mice (control; $85.1 \pm 18.5/3 \times 10^4$ μm^2) ($p < 0.001$). The density of nuclei was calculated in sections stained with thioflavin S and DAPI. The numbers of nuclei in field of 3×10^4 μm^2 were counted at a magnification of ×50

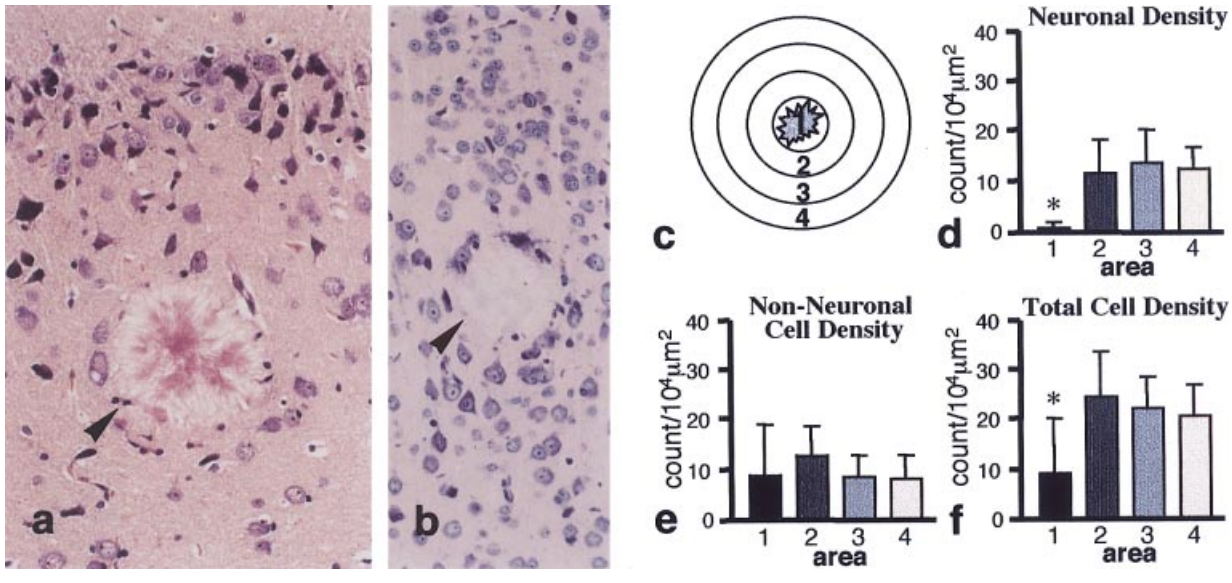

Figure 2. Double staining with Nissl and Congo red (a) and staining with Giemsa dye (b) of the temporal cortex of 18-month-old Tg2576 mice. Neuronal and non-neuronal cell densities were calculated by double staining with Nissl and Congo red (c–f). (a) Neurons were not detected by Nissl staining in or around the amyloid core labelled with Congo red (arrow-head). No cells were found in the core plaque area. The appearance of neurons was preserved without significant compression by the amyloid core. (b) Neurons were not observed in the amyloid core by Giemsa staining (arrow-head). (c) Neurons and non-neuronal cells were counted separately in each of a series of four concentric areas around the amyloid core. The innermost circle circumscribed the amyloid core. The fourth circle extended four core radii from the centre of the amyloid core. The innermost area was area 1 and the outermost area was area 4. (d) Neuronal density in core plaques and other areas of the Tg2576 brain. The neuronal density in area 1 was significantly decreased compared with areas 2–4 ($p < 0.001$). No significant differences were observed among areas 2–4. (e) Non-neuronal cell density in core plaques and other areas of the Tg2576 brain. The number of non-neuronal cells did not show any significant focal reduction around the amyloid cores among these four areas. (f) Total cell density in the Tg2576 brain. The total cell density in area 1 was significantly decreased compared with areas 2–4 ($p < 0.001$), suggesting the focal reduction of neurons in the amyloid cores

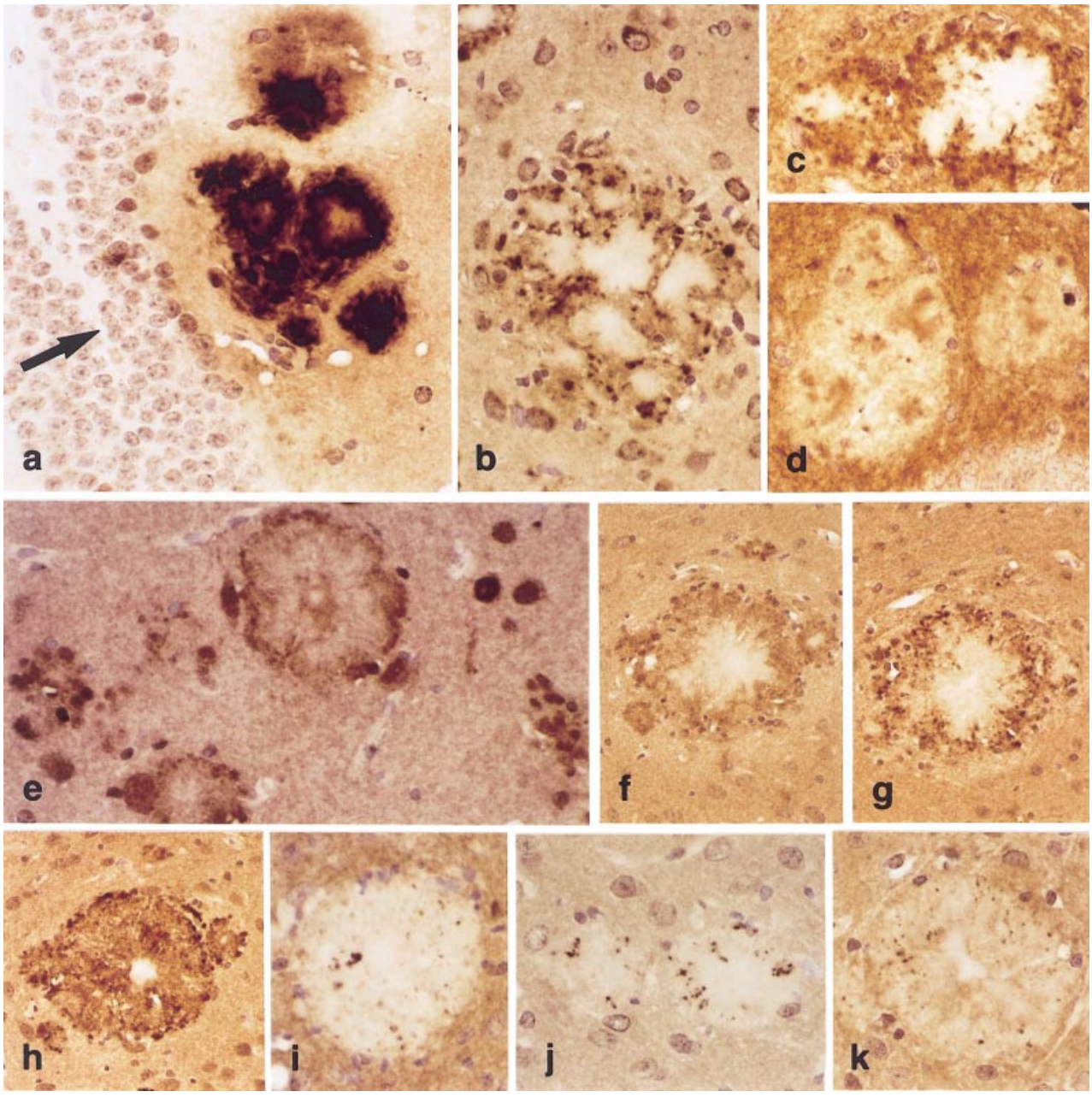

Figure 3. Immunocytochemical findings of the Tg2576 brain stained with antibody Mizuho (a), antibody Saeko (b), NACPC (c), M2F6 (d), HS-C (e), HSN-2 (f), HS-L292 (g), anti-ubiquitin antibody (h), anti-PS199 (i), anti-PS396 (j), and anti-PS413 (k). (a) Anti-Aβ antibody Mizuho labelled small clustered core plaques in the brains of 18-month-old mice. No neurons were observed within the amyloid cores. The loss of granular cells without a compressed appearance was detected in the vicinity of the cores in the dentate gyrus of the hippocampus (arrow). (b) Anti-βAPP antibody Saeko did not label amyloid cores. Marginal dystrophic neurites were intensely stained. (c) NACPC labelled marginal dystrophic neurites. Immunoreactivity with NACPC was absent in the amyloid core. (d) Antibody M2F6 did not show any postsynaptic immunoreactivity in the amyloid core. (e–g) PS-1 immunostaining. HS-C (e), HSN-2 (f), and HS-L292 (g) labelled marginal dystrophic neurites of core plaques, but the amyloid core itself was not stained. (h) Anti-ubiquitin antibody labelled both marginal dystrophic neurites and amyloid cores. (i–k) Phosphorylated tau immunostaining. Anti-PS199 (i), anti-PS396 (j), and anti-PS413 (k) showed dot- and thread-like labelling of a small subset of dystrophic neurites detected by antibody Saeko, HS-C, HSN-2, and HSL-292

Anti-βAPP antibody Saeko staining showed higher levels of expression of βAPP in neurons and their processes in the Tg2576 brain [14]. In the core plaques, this homogeneous expression pattern was absent and no cellular components were recognized. The amyloid cores themselves were not labelled by antibody Saeko. Prominent dystrophic neurites with accumulation of βAPP were observed in and around the core plaques (Figure 3b). Approximately 93% of the core plaques were accompanied by dystrophic neurites with βAPP.

To analyse whether the amyloid core induced synaptic disappearance in the Tg2576 brain, we performed immunostaining for two synaptic proteins, presynaptic α-synuclein [15] and postsynaptic drebrin [10]. The punctate distribution of α-synuclein detected by antibodies NACPN and NACPC was clearly absent

in the amyloid core. Dystrophic neurites in and around the core plaques were also labelled by these two antibodies (Figure 3c). No Lewy bodies were detected in the Tg2576 brain [16]. Although anti-drebrin antibody M2F6 showed dot-like synaptic staining in the cortices, focal disappearance of drebrin was observed in amyloid cores in the Tg2576 brain (Figure 3d).

Since widespread accumulation of C-terminal fragments of PS-1 with NFTs has been reported in the AD brain [6], we examined whether Aβ amyloidosis induced PS-1 accumulation in the Tg2576 brain. Antibodies HS-C, HSN-2, and HS-L292 labelled the cytoplasm and processes of neurons in the brains of these mice [6]. However, antibody HS-C labelled many dystrophic neurites in and around the core plaques in the Tg2576 brain (Figure 3e). Both antibodies HSN-2 and HS-L292 labelled the same dystrophic neurites as HS-C (Figures 3f and 3g). Amyloid core and diffuse plaques were not labelled by HS-C, HSN-2 or HS-L292.

Almost all the dystrophic neurites and the amyloid core were labelled by anti-ubiquitin antibody, suggesting that substances accumulated in dystrophic neurites and plaque core amyloid were ubiquitinated in the Tg2576 brain (Figure 3h).

Antibodies specific to phosphorylation sites of tau, anti-PS199 (Figure 3i), anti-PT205, anti-PT231PS235, anti-PS396 (Figure 3j), and anti-PS413 (Figure 3k), showed dot- or thread-like labelling of dystrophic neurites in the core plaques. The levels of immunoreactivity with anti-PT205 and anti-PT231PS235 were weak. All structures detected corresponded to a small population of dystrophic neurites including PS-1 and ubiquitin.

Discussion

Brain Aβ amyloidosis in the Tg2576 brain was characterized by giant amyloid core plaques. Double staining with DAPI and thioflavin S showed the disappearance of nuclei in and around the core plaques ($p<0.001$). These observations suggested that the amyloid cores substitute for normal brain tissue, develop, and might consequently cause neuronal loss. To confirm these findings, neurons were labelled by Nissl plus Congo red staining. The number of neurons was significantly decreased in the amyloid cores ($p<0.001$). Around the amyloid cores, neurons did not show significant compression and their numbers were not increased. The same findings were obtained by examination using Giemsa staining (data not shown). These three different methods confirmed that neurons were replaced by the amyloid cores in the Tg2576 brain. Some hippocampal neurons disappeared, although they were distant from the giant core plaques. Amyloid cores in the Tg2576 brain might not only replace brain tissue, but could also have the potential to induce focal neuron loss. We also counted neurons in the diffuse plaque and small areas of Aβ deposition without amyloid cores in the Tg2576 brain. These diffuse plaques and small Aβ deposits consisted of non-fibrillar low-molecular-weight β-protein deposits [17] and were detected by methenamine silver staining and immunostaining for Aβ. In contrast to amyloid cores, diffuse plaques and small Aβ deposits did not cause neuronal loss. These findings suggested that neuronal damage in the Tg2576 brain was mainly due to amyloid cores and not to toxicity of low-molecular-weight β-protein deposits [18,19].

Next, to confirm further the tissue substitution and to demonstrate dystrophic neurite formation, sections were stained with anti-βAPP antibody Saeko. No cellular components were detected in the amyloid core and distinct dystrophic neurites were observed in and around all the core plaques. The occurrence of these βAPP-positive dystrophic neurites is a well-known pathological change in the AD brain, suggesting that the disturbed expression of βAPP and its accumulation in damaged neurites were induced by amyloid deposition [14]. Our experiments showed the presence of these βAPP-positive dystrophic neurites in the Tg2576 brain. Thus, tissue substitution and dystrophic neurite formation occurred in the Tg2576 brain as secondary steps in the pathological cascade.

To analyse whether the amyloid core induced synaptic loss in the Tg2576 brain, we performed immunostaining for two synaptic proteins, presynaptic α-synuclein [15] and postsynaptic drebrin [10]. Drebrin is a postsynaptic protein related to synaptic plasticity. In the AD brain, drebrin is selectively decreased to a greater extent than synaptophysin [10]. In the Tg2576 brain, both pre- and post-synaptic proteins, α-synuclein and drebrin, were absent in the core plaques. Thus, Aβ amyloid deposition in the Tg2576 brain had characteristics of brain Aβ amyloidosis, since it replaced both neurons and synapses. These disturbances may contribute to the abnormal behaviour of Tg2576 mice, in addition to dystrophic neurite formation [2].

In the AD brain, aggregated C-terminal fragments of PS-1 are closely related to cytoskeletal abnormalities. Mutant PS-1 is a major cause of familial AD, which alters γ-secretase activity, resulting in an increase in Aβ42(43) to foster Aβ amyloid deposition [1]. It has been reported that PS-1 is either a unique diaspartyl cofactor for γ-secretase, or is γ-secretase itself [20]. PS-1 is present in the endoplasmic reticulum, Golgi compartment, and synaptic vesicles [21,22]. Our experiments showed the accumulation of PS-1 in dystrophic neurites in and around core plaques in the Tg2576 brain. Since the accumulation of PS-1 in dystrophic neurites was identical to that of βAPP and α-synuclein, PS-1 was considered to accumulate in abnormally swollen presynaptic terminals. These findings corresponded to the accumulation of PS-1 C-terminal fragments in dystrophic neurites in the AD brain [6]. Transgenic mouse lines overexpressing mutant PS-1 did not show Aβ deposition or dystrophic neurite formation [23]. These findings indicated that Aβ

amyloidosis induced secondary accumulation of PS-1 in dystrophic neurites. Marked damage by Aβ amyloidosis may cause more extensive accumulation of PS-1 in neuronal processes and cell bodies during longer periods, leading to cytoskeletal abnormalities in the AD brain [6].

Finally, secondary tauopathy induced by Aβ amyloidosis was examined. Ubiquitin, another component of NFTs, also accumulated in the dystrophic neurites in and around the core plaques. To determine whether Aβ amyloidosis induced hyperphosphorylation of tau, five independent phosphorylation sites, Ser199, Thr205, Thr231/Ser235, Ser396, and Ser413, were analysed. These phosphorylation sites were specific to hyperphosphorylated tau in the AD brain [7,8]. Our experiments showed that all of these sites were phosphorylated in the dystrophic neurites in the core plaques in the Tg2576 brain, corresponding to those in the dystrophic neurites in the AD brain. These findings suggested that hyperphosphorylated tau appeared as a secondary event induced by Aβ amyloidosis in the Tg2576 brain.

Previous transgenic mouse studies, including Tg2576, PDAPP, and APP23 mice, did not demonstrate all of these secondary events, although various combinations have been reported. PDAPP mice showed some synaptic loss in the hippocampus and the cerebral cortex, although it was not associated with amyloid plaques [24,25]. APP23 mice showed neuronal loss, potentially induced by amyloid plaques [26,27]. In Tg2576 mice, a slight decrease in the number of neurons in the hippocampus was observed, corresponding to their amyloid burden, but this decrease was not statistically significant. The core plaques covered 4–8% of the 16-month-old Tg2576 mouse hippocampus and cortex [3]. No transgenic mice lines reported to date have shown NFT formation in neurons at light or electron microscopic levels, although phosphorylated tau has been shown to be closely associated with amyloid plaques. We therefore focused on which secondary events are potentially induced by amyloid plaques. We demonstrated here that major stages of the Aβ cascade, i.e. neuronal and synaptic disappearance, PS-1 accumulation, and secondary tauopathy, were induced in the Tg2576 brain, although these alterations were limited to the areas around the core plaques. From this point of view, neuronal loss in the Tg2576 brain should be evaluated as a function of core plaques, not amyloid burden, as performed by Hyman's group. The differences in methodology used might explain why they failed to show neuronal loss in the Tg2576 brain. Our findings clearly indicated that brain Aβ amyloidosis has a potential role in such secondary changes. More extensive accumulation of Aβ amyloid may develop over longer periods, spreading these focal changes throughout the cortices and inducing NFTs. Double transgenic mice produced by crossing Tg2576 with mutant PS-1 or mutant tau mice should lead to a better understanding of the next steps leading to tauopathy and neuronal loss. Answers to the 'Aβ amyloid hypothesis' regarding the pathological role of Aβ amyloidosis and its cascades occurring in the AD brain will be clarified in further studies using these transgenic mouse models.

Acknowledgements

This study was supported by the Life Science Foundation, the Uehara Memorial Foundation, the Univers Foundation, the Sasakawa Health Science Foundation, the Primary Amyloidosis Research Committee, and the Longevity Science Committee of the Ministry of Health and Welfare of Japan and Ministry of Education, Science, and Culture of Japan (12670592, 12670593). We are grateful to Dr Karen Hsiao Ashe for providing Tg2576 mice.

References

1. Scheuner D, Eckman C, Jensen M, *et al*. Secreted amyloid β-protein similar to that in the senile plaques of Alzheimer's disease is increased *in vivo* by the presenilin 1 and 2 and βAPP mutations linked to familial Alzheimer's disease. *Nature Med* 1996; **2**: 864–870.
2. Hsiao K, Chapman P, Nilsen S, *et al*. Correlative memory deficits, Aβ elevation, and amyloid plaques in transgenic mice. *Science* 1996; **274**: 99–102.
3. Irizarry MC, McNamara M, Fedorchak K, Hsiao K, Hyman BT. APPSw transgenic mice develop age-related Aβ deposits and neuropil abnormalities, but no neuronal loss in CA1. *J Neuropathol Exp Neurol* 1997; **56**: 965–973.
4. Kawarabayashi T, Shoji M, Sato M, *et al*. Accumulation of β-amyloid fibrils in pancreas of transgenic mice. *Neurobiol Aging* 1996; **17**: 215–222.
5. Harigaya Y, Shoji M, Kawarabayashi T, *et al*. Modified amyloid β protein ending at 42 or 40 with different solubility accumulates in the brain of Alzheimer's disease. *Biochem Biophys Res Commun* 1995; **211**: 1015–1022.
6. Tomidokoro Y, Ishiguro K, Igeta Y, *et al*. Carboxyl-terminal fragments of presenilin-1 are closely related to cytoskeletal abnormalities in Alzheimer's brains. *Biochem Biophys Res Commun* 1999; **256**: 512–518.
7. Ishiguro K, Sato K, Takamatsu M, Park J, Uchida T, Imahori K. Analysis of phosphorylation of tau with antibodies specific for phosphorylation sites. *Neurosci Lett* 1995; **202**: 81–84.
8. Ishiguro K, Ohno H, Arai H, *et al*. Phosphorylated tau in human cerebrospinal fluid is a diagnostic marker for Alzheimer's disease. *Neurosci Lett* 1999; **270**: 91–94.
9. Shoji M, Harigaya Y, Sasaki A, *et al*. Accumulation of NACP/α-synuclein in Lewy body disease and multiple system atrophy. *J Neurol Neurosurg Psychiatry* 2000; **68**: 605–608.
10. Harigaya Y, Shoji M, Shirao T, Hirai S. Disappearance of actin-binding protein, drebrin, from hippocampal synapses in Alzheimer's disease. *J Neurosci Res* 1996; **43**: 87–92.
11. Yamaguchi H, Haga C, Hirai S, Nakazato Y, Kosaka K. Distinctive, rapid, and easy labeling of diffuse plaques in the Alzheimer brains by a new methenamine silver stain. *Acta Neuropathol* 1990; **79**: 569–572.
12. Sato M, Kawarabayashi T, Shoji M, *et al*. Neurodegeneration and gliosis in transgenic mice overexpressing a carboxy-terminal fragment of Alzheimer amyloid-β protein precursor. *Dementia* 1997; **8**: 296–307.
13. Frautschy SA, Yang F, Irrizarry M, *et al*. Microglial response to amyloid plaques in APPsw transgenic mice. *Am J Pathol* 1998; **152**: 307–317.
14. Shoji M, Hirai S, Yamaguchi H, Harigaya Y, Kawarabayashi T. Amyloid β-protein precursor accumulates in dystrophic neurites

of senile plaques in Alzheimer-type dementia. *Brain Res* 1990; **512**: 164–168.
15. Iwai A, Masliah E, Yoshimoto M, *et al*. The precursor protein of non-Aβ component of Alzheimer's disease amyloid is a presynaptic protein of the central nervous system. *Neuron* 1995; **14**: 467–475.
16. Lippa CF, Fujiwara H, Mann DMA, *et al*. Lewy bodies contain altered α-synuclein in brains of many familial Alzheimer's disease patients with mutations in presenilin and amyloid precursor protein genes. *Am J Pathol* 1998; **153**: 1365–1370.
17. Verga L, Frangione B, Tagliavinin F, Giaccone G, Migheli A, Bugiani O. Alzheimer patients and Down patients: cerebral preamyloid deposits differ ultrastructually and histochemically from the amyloid of senile plaques. *Neurosci Lett* 1989; **105**: 294–299.
18. Kuo Y-M, Emmerling MR, Vigo-Pelfrey C, *et al*. Water-soluble Aβ (N-40, N-42) oligomers in normal and Alzheimer disease brains. *J Biol Chem* 1996; **271**: 4077–4081.
19. Roher AE, Chaney MO, Kuo Y-M, *et al*. Morphology and toxicity of Aβ-(1-42) dimer derived from neuritic and vascular amyloid deposits of Alzheimer's disease. *J Biol Chem* 1996; **271**: 20631–20635.
20. Wolfe MS, Xia W, Ostaszewski BL, Diehl TS, Kimberly WT, Selkoe DJ. Two transmembrane aspartates in presenilin-1 required for presenilin endoproteolysis and γ-secretase activity. *Nature* 1999; **398**: 513–517.
21. Kovacs DM, Fausett HJ, Page KJ, *et al*. Alzheimer-associated presenilins 1 and 2: neuronal expression in brain and localization to intracellular membranes in mammalian cells. *Nature Med* 1996; **2**: 224–229.
22. Efthimiopoulos S, Floor E, Georgakopoulos A, *et al*. Enrichment of presenilin 1 peptides in neuronal large dense-core and somatodendritic clathrin-coated vesicles. *J Neurochem* 1998; **71**: 2365–2372.
23. Duff K, Eckman C, Zehr C, *et al*. Increased amyloid-β42(43) in brains of mice expressing mutant presenilin 1. *Nature* 1996; **383**: 710–713.
24. Games D, Adams D, Alessandrini R, *et al*. Alzheimer-type neuropathology in transgenic mice overexpressing V717F β-amyloid precursor protein. *Nature* 1995; **373**: 523–527.
25. Chen KS, Masliah E, Grajeda H, *et al*. Neurodegenerative Alzheimer-like pathology in PDAPP 717V→F transgenic mice. In *Progress in Brain Research, Vol. 117, Neuronal Degeneration and Regeneration: From Basic Mechanisms to Prospects for Therapy*, Van Leeuwen FW, Salehi A, Giger RJ, Holtmaat AJGD, Verhaagen J (eds). Elsevier: Amsterdam, 1998; 327–334.
26. Calhoun ME, Wiederhold K-H, Abramowski D, *et al*. Neuron loss in APP transgenic mice. *Nature* 1998; **395**: 755–756.
27. Sturchler-Pierrat C, Abramowski D, Duke M, *et al*. Two amyloid precursor protein transgenic mouse models with Alzheimer disease-like pathology. *Proc Natl Acad Sci U S A* 1997; **94**: 13287–13292.

